Effect of the thermal storage dimensions on the performances of Solar Photovoltaic-Thermal Systems

Laura Cirrincione[1,2], Cristina Malara[3], Concettina Marino[3], Antonino Nucara[3*], Giorgia Peri[1], Matilde Pietrafesa[3]

[1] *Department of Engineering, University of Palermo, Palermo, Italy*

[2] *Luxembourg Institute of Science and Technology (LIST), ERIN - Environmental Research & Innovation Department, 41 rue du Brill, L-4422 Belvaux, Luxembourg*

[3] *Department of Civil, Energy, Environmental and Material Engineering (DICEAM), "Mediterranea" University of Reggio Calabria, Reggio Calabria, Italy*

* corresponding author: antonino.nucara@unirc.it

Abstract

PV/T panels are innovative systems increasingly used in the building sector. As a matter of fact, in that context they allow a set of common problems to be addressed and often solved: lack of physical space and economic issues, always existing when PV and thermal panels are to be installed separately.

Obviously, the main objective of PV/T panels is to enhance the electrical efficiency by cooling the PV cells, but the side positive effect is also the production of thermal energy, which can be suitably exploited with a proper configuration of the whole system and an appropriate design of its components.

Their energy production and overall efficiency depend on several factors and therefore the effect of different system features should be investigated. In this work, a parametric analysis was performed to provide a contribution on this topic. The effects of the characteristics of the thermal storage on electrical and thermal system performances were analysed, also considering the influence of the thermal load magnitude.

The conclusive considerations can be exploited by designers and researchers to maximize the efficiency of the systems in relation to the storage tank characteristics and both electrical and thermal loads.

Keywords

Solar energy; Photovoltaic-Thermal (PV/T) Systems; Thermal storage.

1 Introduction

Nowadays, the energy policy of any country tries to address a plurality of issues such as energy security, economic growth and environment protection [1].

Considering these points of view, Renewable Energy Sources, appear to be a valid solution able to flank or, in particular situations, to substitute fossil fuels entirely. Actually, the renewable energy sources are used to supply only 14% of the world's total energy consumption [2]; likely, however, their role is bound to increase because of the rise in fossil fuel prices, global warming and planetary pollution issues.

Solar energy, among all other available energy resources, may be considered as the most abundant, inexhaustible and cleanest. Consequently, the installed area of solar technologies around the world is progressively increasing [3] with a remarkable pace, owing to the unlimited potential available in solar energy.

Many researchers around the world are developing systems based on solar energy [4,5]. The major applications of solar energy can be classified into two categories: solar thermal systems, which convert solar energy into thermal energy, and photovoltaic (PV) systems, which convert solar energy into electrical energy. These systems are usually used separately.

As regards PV cells, by and large, it is acknowledged that their output decreases when the operating temperature increases. Thus, in order to have a better performance, it is crucial to maintain the operating temperature values of the solar cells as low as possible [6,7], also considering the weather conditions of the site.

Therefore, in order to achieve a higher electrical efficiency, the PV module should be cooled by removing the heat, for instance exploiting the performance of a coupled solar air/water heater collector. The resulted combined system is called solar photovoltaic thermal (PV/T) collector and is able to produce thermal and electrical energy simultaneously. Apart from the twofold energy performance, the advantage of the PV/T system consists in the reduction of the demand of physical space as compared to the separated PV and solar thermal systems placed side-by-side.

These features make PV/T systems suitable for building installations, where the problem of limited usable shadow-free space on building rooftops is the key issue. Consequently, PV/T collectors are currently considered as a valid contribution to the actual implementation of the nearly Zero Energy Buildings (nZEB) concept [8–10].

A significant amount of theoretical [11,12] and experimental studies [13] on the PV/T systems has been carried out in the last few years, so that PV/T modules have been variously modelled [14,15]. The main purpose of these analyses was to explore the main factors influencing the electric and thermal performances of the systems.

As a matter of fact, albeit PV/T modules are cogenerating systems, producing both electric and thermal energy, hardly can their performances be optimized from all the functional perspectives (heat and electric energy conversion), so that, for the same operating conditions, single PV or thermal panels may be characterized by a higher efficiency in their correspondent function [16].

Within this framework, a remarkable number of the available studies focus on the PV/T features, with a view to analysing the influence of specific parameters [17] and designing efficient configurations [18–20] also depending on the used materials [21]. In addition, specific tools capable of simulating hybrid solar collectors were also devised [22,23]

Most of the cited studies, however, regard the panel specific features, constitutive materials and performances, without any reference to the structure or configuration of the plant, which they are usually part of.

As far as the integration of PV/T panels into plants and systems, the majority of research regards the analysis of specific configurations. For instance, a trigeneration system (PV/T plus absorption chiller) is analysed in [24] where a simulation tool was exploited to assess the energy savings for a specific case study with fixed loads. A sensitive analysis also demonstrated that for the studied case the results are dramatically sensitive to the variations of the PV/T area, whereas the other parameters (tank volume, fluid set point temperatures, and flow rate) slightly affect the overall results.

A case study with fixed loads (thermal and electric) was also considered in [25] where thermo-economic optimization of a specific solar system (for a specific range of design parameters involving the number of concentrated photovoltaic/thermal collectors, the number of PV collectors, the number of evacuated tube collectors, the volume of the storage tank, and the battery capacity) was performed.

The real buildings' energy demands of the University campus of Bari were also used as input to a transient system model in [26]. The system was a solar combined cooling, heating and power one based on hybrid PV/T modules. In the study, the water storage tank was modelled exploiting the same simulation procedure described in [27], where a temperature stratification was considered and an analysis regarding the influence of the storage volume on the energy and economic performance of a solar combined heat and power system was carried out. In this case, the specific electric and thermal loads of three reference buildings, each typical of three locations,

characterized by diverse climate conditions, were used. The system components (e.g. number of modules, water tank volume, etc.) were dimensioned for each reference household.

To sum up, the majority of the available research refers to either the optimization of the PV/T module features and configurations or the analysis of the energy and economic performance of specific system structures, when called to meet specific loads also in different climate conditions. Therefore, an important contribution to the topic could be delivered by studies either addressing the issue of how the configuration and size of the system components may be arranged to meet different loads or aiming at the assessment of the thermal loads, which might be efficiently met by a specific system configuration.

In this context, the perspective of the proposed analysis regards the assessment of the thermal loads whose magnitude might be effectively satisfied by the proper system, depending on the water storage features, namely the tank size and thermal transmittance.

Specifically, the parametric analysis performed in this paper aims to provide indications about the effect of the combined interaction of the storage system features (size and thermal transmittance) and the thermal load magnitude on the temperature of the working fluid and, therefore, on the actual viability of the system.

The focus is also on the thermal losses from the storage tank and on the possibility of their exploitation to enhance the performance of the PV/T module, while preventing thermal storage temperature from dropping remarkably.

Therefore, the analysis is also devoted to the quality of the thermal energy attainable and not only to its global amount.

On the other hand, if a water temperature drop is inevitable in order to guarantee acceptable performances from the PV energy conversion point of view, the parametrical analysis reported in the presented article aims to single out the loads that could be better met in any of the examined cases.

These indications can be exploited by designers and researchers, to maximize the efficiency of the systems in relation to both the thermal load magnitude and the features of the water thank.

With a view to fulfilling the task, a simulation model was designed and implemented in a Visual Basic™ environment.

For the sake of simplicity, the model was designed with a view to maintaining a viability and an easiness of use, in order to possibly perform all the needed simulations swiftly, albeit keeping an acceptable level of accuracy, also considering that the focus of the analysis involves comparison purposes.

Several features of the system components were patterned and simulated in order to examine the effect of the characteristics of the thermal storage on both system's electrical and thermal performances; they vary for the thermal load magnitude and for both the thermal insulation properties and dimensions of the tank used for thermal storage purposes.

2 Methodology

The article presents the results of a parametric analysis focused on the assessment of the influence of both thermal storage features and thermal load size on the performance of photovoltaic-thermal systems, in order to single out the context and the constrains of their possible suitability.

Specifically, the aim is to investigate about the effect of the combined interaction of the storage system features (size and thermal transmittance) and the thermal load magnitude on the temperature of the working fluid and, therefore, on the actual suitability of the system.

From this perspective, as a matter of fact, the thermal losses might also be exploited with a view to striking a balance between the needs of improving both the photovoltaic conversion efficiency by cooling the PV

module and the production of suitable thermal energy. In order to fulfil this task, the water storage tank should be designed properly.

The analysis proposed in the article focuses on this aspect of the issue, also regarding the quality of the produced thermal energy; to reach this aim, a simple model has been designed. It simulates the system behaviour in transient regime and is based on the lumped parameter model reported in [28], modified to take the effect of the PV module into account.

The steps of the whole procedure are synthetized in the flow-chart of Fig. 1, and described in the following sections.

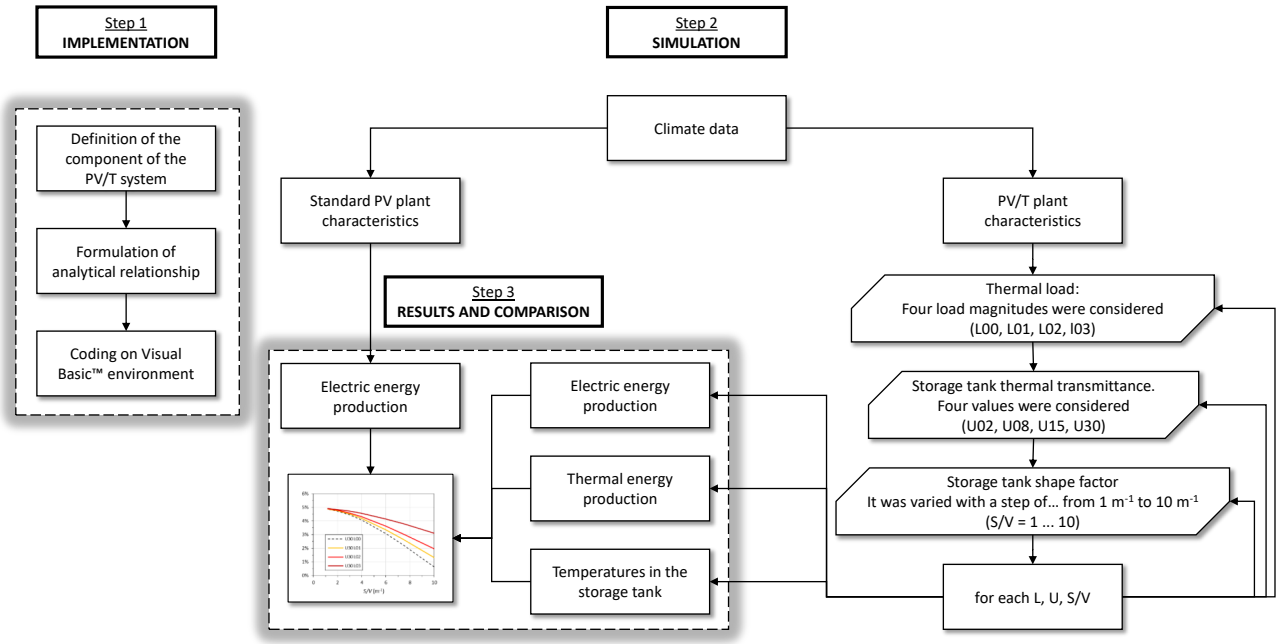

Fig. 1. Flow-chart of the methodology.

Firstly, a pattern of a typical system was designed, considering the main constitutive elements (hybrid panels, pumps, thermal storage, expansion tank, etc, Fig.2), and successively the plant operation was modelled by implementing, in a Visual Basic™ environment, proper relationships describing the various involved physical phenomena (e. g. photovoltaic conversion and heat exchanges) and their interaction.

Several features of some system components were patterned and simulated; they vary for the thermal load size and for both the thermal insulation properties and dimensions of the tank used as thermal storage.

Discussed results regard both the yearly electric and thermal energy production, the water temperature of the thermal storage and the persistence of water temperature values suited to satisfy the thermal load requisites or, alternatively, to provide support to an auxiliary heating source.

In order to facilitate comparisons among outcomes of different systems configurations, all the energy amounts resulted from the simulations were referred to the annual electric energy production derived from a simple photovoltaic system working at the same conditions of the actual analysed plant. Specifically, the following indicators were evaluated:

– the ratio of the electrical energy production due to the use of the PV/T system respect to a standard PV one:

$$R_E = \frac{Q_{E,PV/T}}{Q_{E,PV}} \quad (1)$$

– the ratio of the thermal energy production to the electrical energy production of the standard PV system:

$$R_U = \frac{Q_U}{Q_{E,PV}} \quad (2)$$

– the increase of the electric energy production due to the use of the PV/T system with respect to a standard PV one:

$$\Delta_E = \frac{Q_{E,PV/T} - Q_{E,PV}}{Q_{E,PV}} \quad (3)$$

where:

– $Q_{E,PV/T}$ is the annual electrical energy, generated by the PVT panel (Wh);
– $Q_{E,PV}$ is the annual electrical energy, generated by the PV panel characterized by the same features as the studied PV/T one and working at the same conditions (Wh);
– Q_U is the annual available thermal energy, at load disposal (Wh).

In addition, in order to sum up results regarding the energy production, the primary energy saving efficiency, η_p, was also assessed. It is defined as [29]:

$$\eta_p = \frac{\eta_{PV}}{\eta_e} + \eta_T \quad (4)$$

where:

– η_{PV} is the efficiency of the PV panel;
– η_T is the thermal efficiency of the PV/T panel;
– $\eta_e = 0.38$ is the electrical power generation efficiency of the Italian energy system [30].

Furthermore, with a view to assessing the thermal conditions of the water storage, different parameters were considered: the maximum water temperature during the simulation period (one year), $t_{A,max}$, the fraction of time in a year during which the water temperature remains higher than 25°C and 45°C respectively, namely:

$$f_{25} = \frac{\tau(t_A > 25°C)}{8760} \quad (5)$$

$$f_{45} = \frac{\tau(t_A > 45°C)}{8760} \quad (6)$$

where $\tau(t_A > 25°C)$ is the length of the period of time during which the water storage temperature. t_A, is higher than 25°C, whereas $\tau(t_A > 45°C)$ is the length of the period of time during which the water storage temperature. t_A, is higher than 45°C.

3 System Modelling

The proposed simulation model is based on the lumped parameter model reported in [28], modified to take the effect of the PV section into account. It aims at simulating the system behaviour in transient regime.

The system has been patterned considering its main components: photovoltaic module, thermal collector and thermal energy storage system (Fig. 2).

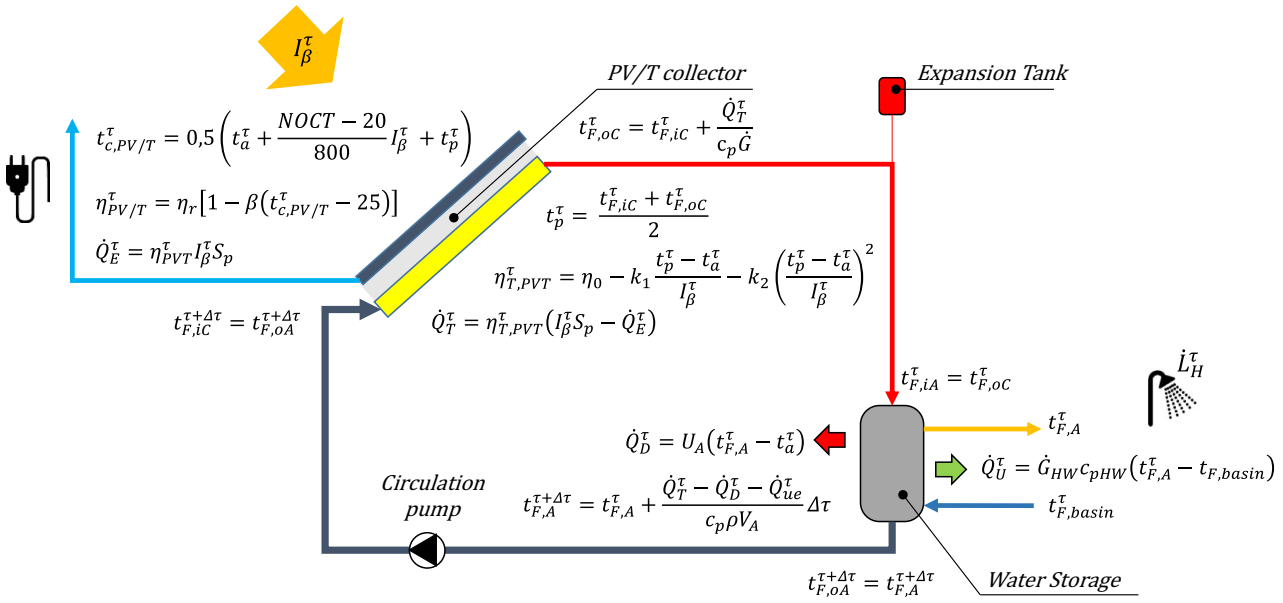

Fig. 2. Scheme of the analysed system.

The energy balance equation of the PV/T panel at time τ is calculated assuming that the amount of solar radiation, which is not involved in the PV conversion, contributes to heating the cooling fluid:

$$\eta_T^\tau\left(I_\beta^\tau S_p - \eta_{PV}^\tau I_\beta^\tau S_p\right) = c_p \dot{G}\left(t_{F,oC}^\tau - t_{F,iC}^\tau\right) \tag{7}$$

where:

- η_T^τ is the thermal efficiency of the PV/T system;
- I_β^τ is the solar irradiance on the panel surface;
- S_p is the panel surface;
- η_{PV}^τ is the efficiency of the PV panel;
- c_p is the specific heat capacity;
- $\dot{G}$ is the water flow in the PV/T panel;
- $t_{F,oC}^\tau$ is the collector outlet water temperature;
- $t_{F,iC}^\tau$ is the collector inlet water temperature.

The thermal efficiency of the PV/T panel may be assessed as a function of the temperature of the absorber plate, t_p^τ, the air temperature, t_a^τ, and the solar irradiance [31]:

$$\eta_T^\tau = \eta_0 - k_1 \frac{t_p^\tau - t_a^\tau}{I_\beta^\tau} - k_2\left(\frac{t_p^\tau - t_a^\tau}{I_\beta^\tau}\right)^2 \tag{8}$$

where η_0, k_1 and k_2 are parameters characterizing the collector.

The temperature of the absorber plate is assumed equal to:

$$t_p^\tau = \frac{t_{F,iC}^\tau + t_{F,oC}^\tau}{2} \tag{9}$$

where $t_{F,iC}^\tau$ e $t_{F,oC}^\tau$ are the collector inlet and outlet water temperature, respectively.

The efficiency of the PV panel can be calculated by means of [31]:

$$\eta_{PV}^\tau = \eta_r\left[1-\beta\left(t_{c,PVT}^\tau - 25\right)\right] \tag{10}$$

with η_r nominal efficiency of the PV panel, β temperature coefficient, and t_c^τ cell temperature.

Therefore, the performance of the system is a function of the cell temperature, $t^{\tau}_{c,PV/T}$, which in turn depends on both the cell temperature of the standard PV panel working at the same condition of the actual one, $t^{\tau}_{c,PV}$, and the thermal collector absorber plate temperature, t^{τ}_{p}. It was assumed that:

$$t^{\tau}_{c,PV/T} = \frac{t^{\tau}_{c,PV} + t^{\tau}_{p}}{2} \tag{11}$$

The assumption was motivated by the following considerations. The possible values of the cell temperature of the PV/T panel are restrained within a range whose limits are: $t_{c,PV}$ and t_p. For the higher inertia of the thermal component of the system (which exploits water as working fluid), it is more likely that the actual temperature of the cell, $t^{\tau}_{c,PV/T}$, is nearer to absorber temperature, t_p, than cell temperature of the simple PV panel. Nonetheless, as a conservative hypothesis from the perspective of electric production, an average value was considered.

The cell temperature of the standard PV system operating at the same condition of the actual PV/T plant, $t_{c,PV}$, is usually calculated by means of the well-known equation [32]:

$$t^{\tau}_{c,PV} = t^{\tau}_{a} + \frac{NOCT - 20}{800} I^{\tau}_{\beta} \tag{12}$$

where $NOCT$ is the Nominal Operating Cell Temperature, t^{τ}_{a} the air temperature and I^{τ}_{β} the solar irradiance on the panel surface.

The collector outlet water temperature, $t^{\tau}_{F,uC}$, is hereafter calculated from eq. (7), by means of the following formula:

$$t^{\tau}_{F,oC} = t^{\tau}_{F,iC} + \frac{\dot{Q}^{\tau}_{T}}{c_p \dot{G}} \tag{13}$$

where:

$$\dot{Q}^{\tau}_{T} = \eta^{\tau}_{T}(I^{\tau}_{\beta} S_p - \dot{Q}^{\tau}_{E}) \tag{14}$$

and

$$\dot{Q}^{\tau}_{E} = \eta^{\tau}_{PV} I^{\tau}_{\beta} S_p \tag{15}$$

The water temperature in the storage system is calculated considering the following energy balance equation [33]:

$$c_p \rho V_A \frac{dt}{d\tau} d\tau = \dot{Q}_g d\tau - \dot{Q}_l d\tau \tag{16}$$

where ρ is the density of the fluid, V_A the storage volume, $\dot{Q}_g$ the energy supply flow, and $\dot{Q}_l$ indicates the thermal losses.

Under the hypothesis that the thermal losses within the water circuit are negligible and assuming that no fluid stratification occurs within the water tank, so that the storage temperature $t_{F,A}$ is uniform [28,33] (perfect mixing hypothesis), it results that:

$$t^{\tau+\Delta\tau}_{F,A} = t^{\tau}_{F,A} + \frac{\dot{Q}^{\tau}_{T} - \dot{Q}^{\tau}_{D} - \dot{Q}^{\tau}_{ue}}{c_p \rho V_A} \Delta\tau \tag{17}$$

where $\dot{Q}^{\tau}_{D}$ is the thermal flow through the envelope structure of the water storage, $\dot{Q}^{\tau}_{ue}$ is the thermal power sent to the thermal load, ρ is the density of the fluid, and V_A is the volume of the storage.

The hypothesis of negligible thermal losses implies that:

$$t_{F,oC}^{\tau} = t_{F,iA}^{\tau} \tag{18}$$

$$t_{F,oA}^{\tau} = t_{F,iC}^{\tau} \tag{19}$$

Therefore, the following equation may be yielded:

$$\dot{Q}_T^{\tau} = \dot{G} c_p \left(t_{F,oA}^{\tau} - t_{F,iA}^{\tau}\right) = \dot{G} c_p \left(t_{F,iC}^{\tau} - t_{F,oC}^{\tau}\right) \tag{20}$$

The thermal flow through the envelope structure of the water storage is calculated by:

$$\dot{Q}_D^{\tau} = U_A (t_{F,A}^{\tau} - t_a^{\tau}) \tag{21}$$

in which U_A is the thermal transmittance of the envelope structure of the water storage.

As regards the effective thermal power, $\dot{Q}_{ue}^{\tau}$, namely the thermal power, which is actually sent to the thermal load, it is calculated considering that, when the thermal energy production exceeds the thermal demand, only the needed portion of the global available thermal power $\dot{Q}_U$ is used to meet the thermal load $\dot{L_H}$.

Therefore:

$$\dot{Q}_U^{\tau} = \dot{G}_{HW} c_p (t_{F,A}^{\tau} - t_{F,basin}) \tag{22}$$

where $\dot{G}_{HW}$ is the water flow of the fluid in demand loop and $t_{F,basin}$ the groundwater temperature, and:

$$\begin{aligned} \dot{Q}_{ue}^{\tau} &= \dot{Q}_U^{\tau} \quad if \quad \dot{Q}_U^{\tau} \le \dot{L}_H^{\tau} \\ \dot{Q}_{ue}^{\tau} &= \dot{L}_H^{\tau} \quad if \quad \dot{Q}_U^{\tau} > \dot{L}_H^{\tau} \end{aligned} \tag{23}$$

Moreover, it is assumed that:

$$\dot{Q}_{ue}^{\tau} = 0 \quad if \quad \dot{Q}_U^{\tau} < 0 \tag{24}$$

Finally, the collector inlet water temperature will be equal to the storage outlet water temperature:

$$t_{F,iC}^{\tau+\Delta\tau} = t_{F,oA}^{\tau+\Delta\tau} = t_{F,A}^{\tau+\Delta\tau} \tag{25}$$

The procedure was implemented in a spreadsheet, using Visual Basic™ function and macros, and a user-friendly interface was designed. The used time step is equal to 6 minutes (10 steps every hour).

At each time step, the climatic parameters, recorded on an hourly basis, were calculated by linear interpolation using the values corresponding to two consecutive hours.

The code output consists of:

- cell temperature $t_{c,PV/T}^{\tau}$;
- inlet and outlet water temperature of the collector, $t_{F,iC}^{\tau}$ and $t_{F,oC}^{\tau}$;
- water storage temperature $t_{F,A}^{\tau}$;
- generated electrical power $\dot{Q}_E^{\tau}$;
- generated thermal energy $\dot{Q}_T^{\tau}$;
- global available thermal power $\dot{Q}_U^{\tau}$;
- effective thermal power $\dot{Q}_{ue}^{\tau}$;
- thermal flow through the envelope structure of the water storage $\dot{Q}_D^{\tau}$;
- electrical efficiency η_{PV}^{τ};
- thermal efficiency η_T^{τ}.

4 Performed Analysis

With the aim of analysing the role of thermal storage structure on the performances of the whole system, several configurations were patterned and simulated; they vary for the thermal load and for both the thermal insulation properties and dimensions of the tank used for thermal storage purposes.

4.1 Climate Data

The studied PV/T system is located in Reggio Calabria, (38°07'12" North latitude, 15°40'12" East longitude), a town situated on the Southern coast of the Italian Peninsula and characterized by a typical Mediterranean climate profile, with mild winter climate and dry warm summer.

The needed climate data were obtained through a measurement campaign performed at the Mediterranean University campus. Solar radiation was measured by means of a Kipp and Zonen CNR4^{TM} net radiometer, whereas the air temperature was measured using the Vaisala WXT 520 weather station. The technical characteristics of the measuring equipment are reported in Table 1 and Table 2. Weather data were measured with an hourly time step, for a whole year.

Table 1. Technical characteristics of CNR4™ net radiometer.

Spectral range	300 - 2800 nm (50% points)
Sensitivity	10 to 20 µV/ (W/m²)
Response time	< 18 s (95% response)
Non-linearity	< 1 % (from 0 to 1000 W/m₂irradiance)
Tilt error	< 1 %
Field of view	180°
Directional error	< 20 W/m² (angles up to 80° with 1000 W/m² beam radiation)
Irradiance	0 to 2000 W/m²
Uncertainty in daily total	< 5% (95 % confidence level)

Table 2. Technical characteristics of Vaisala WXT520.

Measured parameter	Measurement range	Accuracy
Air temperature	-52…+60°C	±0.3°C
Relative Humidity	0-100%	±3% RH
Rain intensity	0-200 mm/h	±0.1 mm/h

The climatic conditions of the site are synthetically depicted in Fig. 3, which reports the values of both the monthly solar radiation on the horizontal plane and the daily average air temperature, obtained from the measured data.

These measured climatic data were used as input to the simulation model, which assesses the values of every parameter in correspondence of each calculation step (equal to 6 minutes) by means of the linear interpolation method.

In addition, the hourly components of the solar radiation shining on the PV/T panel surface were assessed by means of the Liu and Jordan method [34], starting from the knowledge of the measured hourly global solar radiation on the horizontal surface [35].

Measured data allowed the actual climate conditions of the site to be taken into account, especially as far as solar radiation is concerned [36].

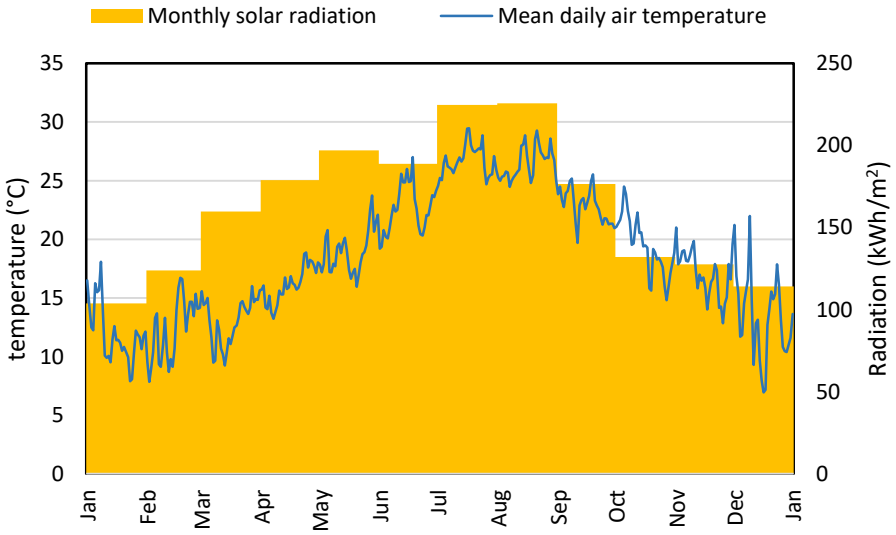

Fig. 3. Monthly solar radiation on the horizontal plane and daily average air temperature.

4.2 Thermal load

Four constant thermal loads, L_H, were considered; their amounts are reported in Table 3.

Specifically, in Table 3, the yearly thermal demand $L_{H,y}$ is conveyed as a function of the yearly electric production, $Q_{E,PV}$, of the PV system working at the same conditions of the actual PV/T:

$$\boldsymbol{L_{H,y}} = Q_{E,PV,y} \times k \tag{26}$$

with $k = 0.0; 0.5; 1.0; 2.0$.

The value of $Q_{E,PV,y}$, assumed as reference, resulted from the simulation of a standard PV system with unitary panel surface.

The constant thermal power instantaneously requested by the load, $\boldsymbol{L_{H,h}}$,was hence calculated by means of the following equation:

$$\boldsymbol{L_{H,h}} = \frac{\boldsymbol{L_{H,y}}}{8760} \tag{27}$$

Table 3. Thermal loads.

Load hypothesis	Yearly thermal energy demand, $\boldsymbol{L_{H,y}}$ (kWh)	Instantaneous thermal load $\boldsymbol{L_{H,h}}$ (W)
L00 → $L_{H,y} = 0$	0	0
L01 → $L_{H,y} = 0.5\ Q_{E,PV,y}$	136	15.5
L02 → $L_{H,y} = Q_{E,PV,y}$	272	31
L03 → $L_{H,y} = 2\ Q_{E,PV,y}$	543	62

The choice of using a constant thermal load profile only relies on the fact that former analyses [37] demonstrated that the result variability due to the thermal load profile (constant or variable) is real, but less significant than the one caused by variation in storage features such as transmittance and shape factor.

Moreover, the aim of the study is to compare the output yielded by different system feature configurations rather than determine an absolute value of energy production. From this perspective, the real issue is that the input data and initial conditions are equal for each simulated configuration.

4.3 PVT panel

The studied PV/T panel consists of a Monocristalline PV module and a sheet and tube absorber. The panel surface is 1 m^2, the electrical and thermal specifications of the system are reported in Table 4.

All the simulations regarded a panel with unitary surface, peak power of 120 W/m^2, facing South and inclined at an angle of 28° to the horizontal plane.

Table 4. PV/T panel technical features.

Electrical specifications			Thermal specifications		
η_r (-)	$NOCT$ (°C)	β (%/°C)	η_0 (-)	k_1 (W/m^2K)	k_2 (W^2/m^4K^2)
0.150	45.0	-0.4	0.500	4.58	0.00135

Solar irradiance on the PV/T surface was calculated by means of the Liu and Jordan method [34], using the measured data on the horizontal plane.

4.4 Storage tank

With a view to evaluating the effect of the characteristics of the thermal storage, several insulation configurations of the tank were considered. The correspondent thermal transmittance values are reported in Table 5; moreover, the simulations were performed for various values of the shape factor, that is the ratio of the surface of the tank envelope, S, to its volume, V.

Table 5. Considered thermal transmittance values of the storage tank.

Case	Thermal transmittance, U (W/m^2K)
U30	3.0
U15	1.5
U08	0.8
U02	0.2

5 Results

Firstly, with a view to giving a preliminary information regarding the obtained results, Fig. 4 and Fig. 5 report the time trend of the water storage temperature, air temperature and solar radiation on the panel surface for a summer week and for a winter week, respectively. Similar results can be obtained for each involved parameter (e.g. cells and fluid temperatures, generated electric and thermal energy, electric and thermal efficiency, etc.)

Specifically, the trends depicted in the two figures refer to a specific case consisting of the following conditions:

- Load configuration L02, $L_{H,h} = 31\ W$;
- Thermal transmittance U30, $U = 3.0\ W/m^2°C$:
- Shape factor $S/V = 6.0\ m^{-1}$.

It can be noted that the water storage temperatures are lower than 35°C also during the June week, and their trend follows the climatic condition variability (air temperature), with a thermal inertia whose effect is visible during the cooling phase starting after sunset; this is in accordance with other findings [26].

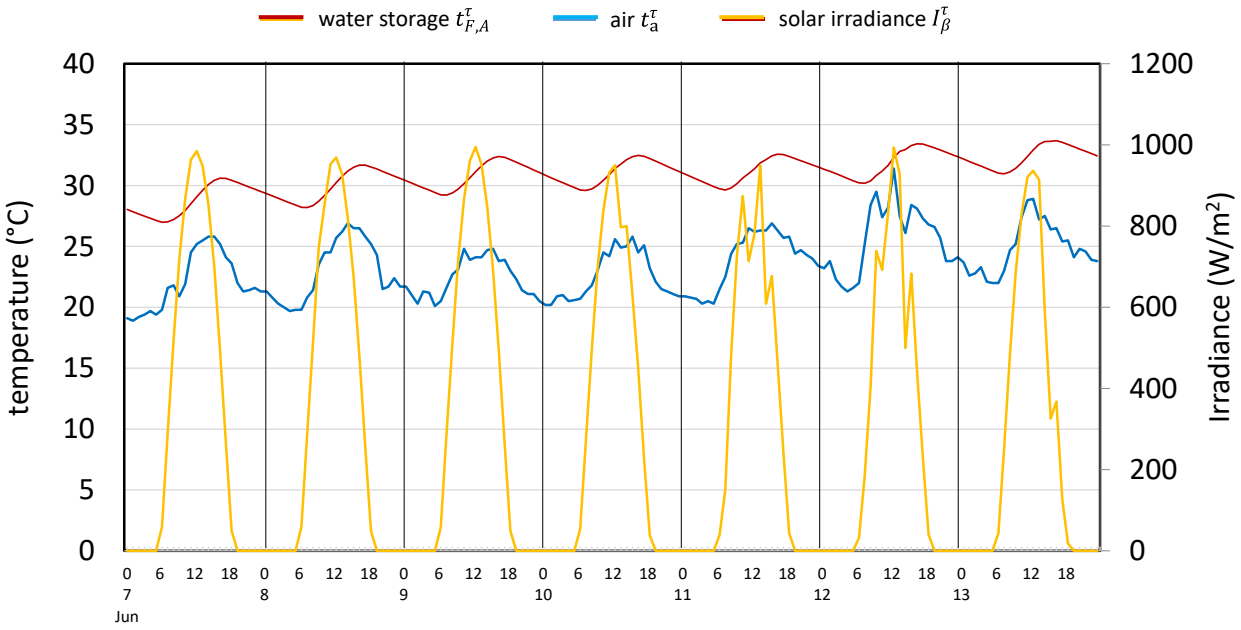

Fig. 4. Time trend of water storage temperature, air temperature and solar radiation on the panel surface (summer week, $\boldsymbol{L_{H,h}} = 31\ W$, $U = 3.0\ W/m^2°C$, $S/V = 6\ m^{-1}$).

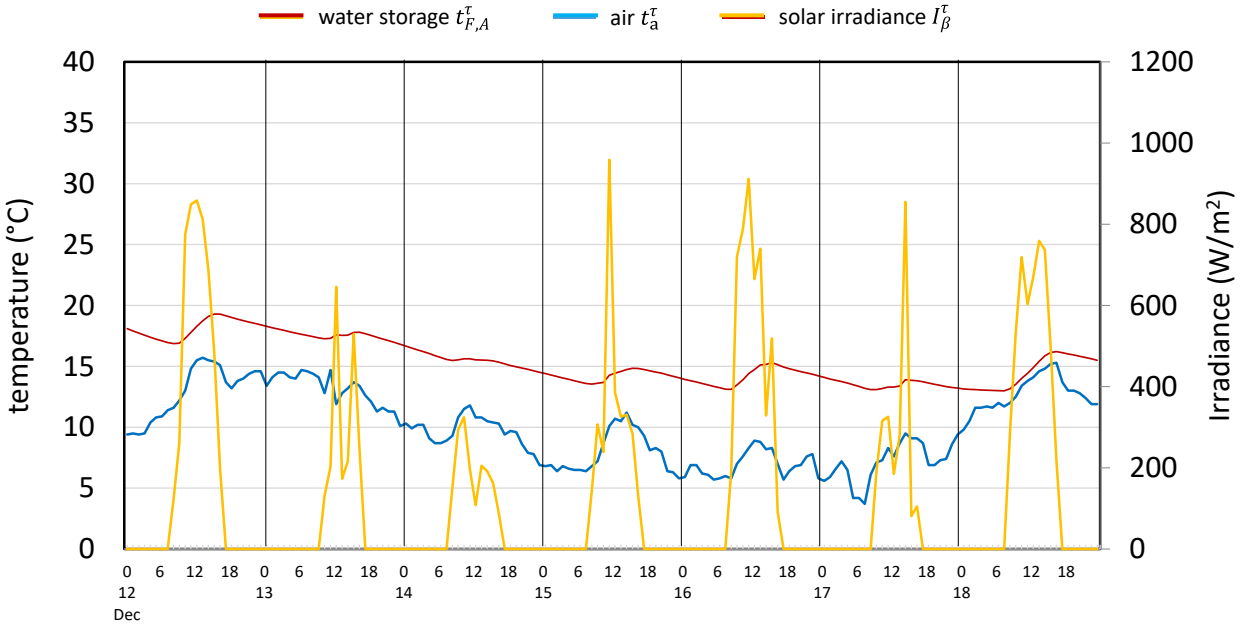

Fig. 5. Time trend of water storage temperature, air temperature and solar radiation on the panel surface (winter week, $\boldsymbol{L_{H,h}} = 31\ W$, $U = 3.0\ W/m^2°C$, $S/V = 6\ m^{-1}$).

Obviously, Fig. 4 and Fig. 5, referring to a single case in a short period of time, can be considered only as an example of the system behaviour. In fact, they give no information regarding both the annual system performance and the effect of the change in the parameter values involved in the parametric analysis.

Actually, results of the parametric analysis, on an annual basis, are depicted in figures from 6 to 16, which summarize the outcomes of the performed simulations as a function of the shape factor, S/V, namely the ratio of the surface of the tank (*i.e.* the heat exchange surface to the outdoor environment), S, to its volume, V. This is an important parameter, which strongly influences the transient behaviour of systems involved in heat transfer processes. Being able to give an account of both the size and thermal response of the water storage, the shape factor was deemed a proper parameter to be used for the parametrical analysis.

Therefore, for all the reported graphs, the shape factor is the X-axis variable. Its values depend on the geometrical dimensions of the tank; the larger the storage is, the smaller the shape factor is.

Specifically, the figures depict the trends of:

- the increase of the electric energy production due to the use of the PV/T system respect to a standard PV one, Δ_E;
- the ratio of the thermal energy production to the electrical energy production of the standard PV system, R_U;
- the maximum yearly water temperature in the storage tank, $t_{A,\max}$;
- the fraction of time during which the water temperature in the storage tank remains higher than 25°C and 45°C, respectively, namely f_{25} and f_{45}.

In Fig. 6 and Fig. 7, the yearly increase of the electric energy production due to the cooling of the PV system is reported.

It can be inferred that, the highest increase Δ_E in the energy production always occurs in correspondence of the lowest values of the shape factor (largest storage volume).

For $S/V < 1.8\ m^{-1}$ it was found $4\% < \Delta_E < 5\%$, regardless the values of the involved parameters (load magnitude, tank transmittance).

In addition, Δ_E, whose values never exceed 5%, always decreases when the shape factor increases. The rate and shape of this decreasing trend depend on the thermal load and the thermal transmittance of the tank.

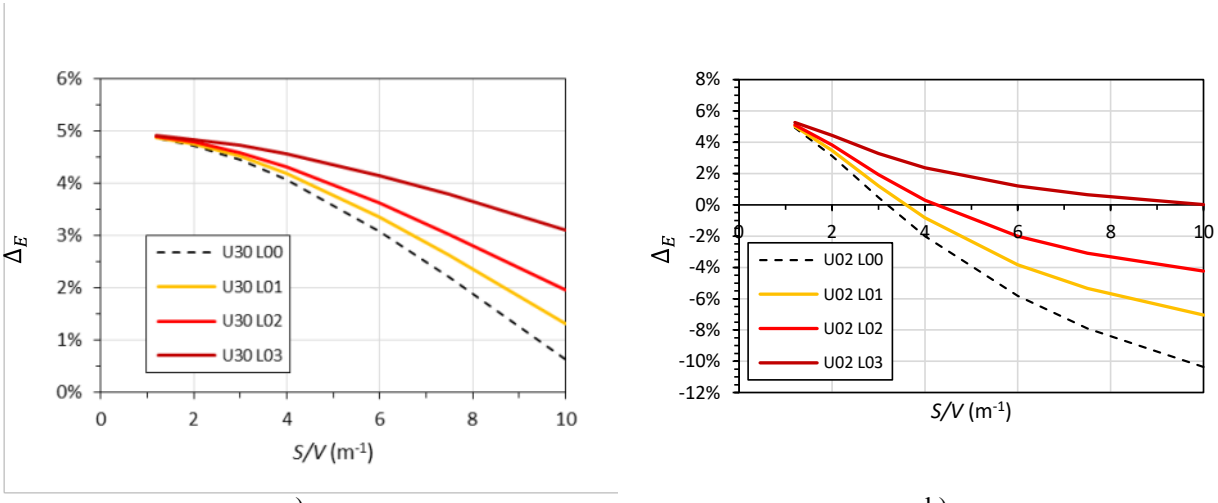

a) b)

Fig. 6. Electric energy production increase, Δ_E, for various load conditions:
case a) U=3.0 W/m^{2}K; case b) U=0.2 W/m^2/K.

Specifically, regardless the thermal load values, the gradient of the curve rises with S/V, when the less insulated tank is involved (Fig. 6-a). On the contrary, the same gradient decreases and tends to 0, when the insulation properties of the tank are improved (Fig. 6-b). Moreover, in this latter case (Fig. 6-b), when $S/V > 4\ m^{-1}$, only the presence of the highest thermal load rate ($L_{H,h} = 62\ W$, configuration L03) allowed Δ_E values higher than 0.

The effect of the tank heat loss coefficient is also inferable from Fig. 7, where a change in the curve concavity (from upward to downward), occurring when U increases, is also clearly visible for both the depicted load configurations (L00 and L03).

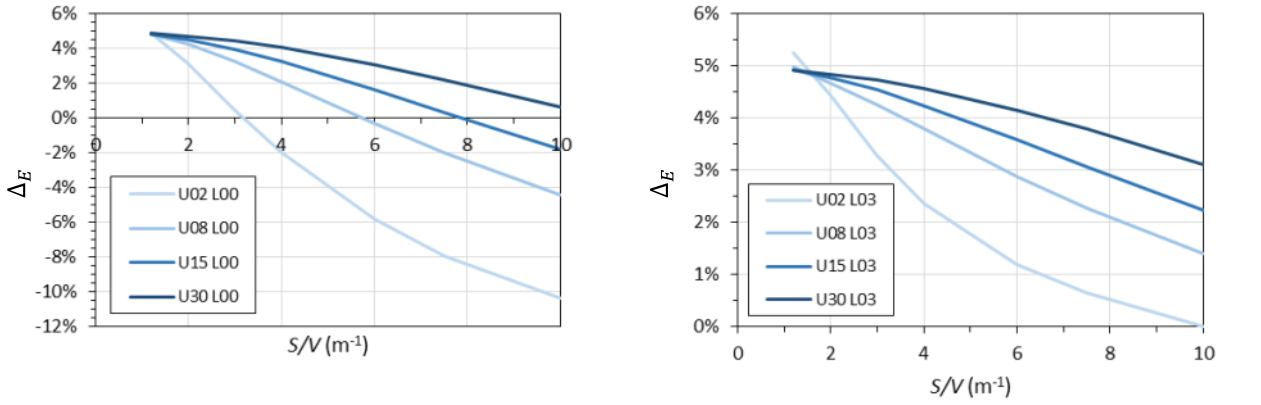

a) b)

Fig. 7. Electric energy production increase, Δ_E, for various trasmittance values of the storage tank: case a) no thermal load; case b) thermal load condition L03.

Similar behaviour regards the thermal energy production and it is depicted in Fig. 8 and Fig. 9, which report the trend of the ratio of the thermal energy production to the electrical energy production of the standard PV system, R_U, versus the shape factor S/V.

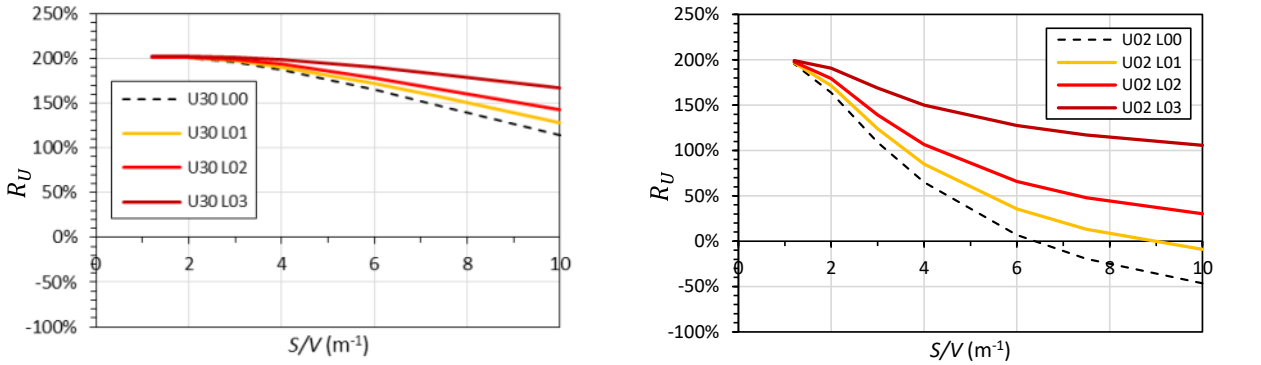

a) b)

Fig. 8. Ratio of the thermal energy production to the electrical energy production of the standard PV system, R_U: case a) U=3.0 W/m^{2}K; case b) U=0.2 W/m^2/K.

It is worthy of note that when the least insulated tank (Fig. 8a, U=3.0 W/m^{2}K) is involved, the improvement of thermal energy production R_U, is almost constant with S/V, for $S/V < 4\ m^{-1}$.

On the contrary, for $S/V > 4\ m^{-1}$ the thermal energy production starts decreasing when S/V rises, for all the considered thermal load configurations.

The decreasing trend, for rising S/V values, always characterizes the results regarding the most insulated tank (Fig. 8b, U=0.2 W/m^{2}K). Moreover, in this case, the curve decrease rate is higher than the one obtained in correspondence of large U-values. In other words, the diminution in energy production, for rising S/V values, becomes significant when the transmittance of the storage tank is low.

Presumably, this occurrence is caused by the effect of the warm climate conditions of the site: for the least insulated tank (U=3.0 W/m^{2}K), the outdoor environment contributes to heating the fluid; this contribution counteracts the effect due to the shape factor increase, so that the trend of the yearly available thermal energy *versus* S/V decreases with a rate lower than the one occurred in correspondence of small U values (U=0.2 W/m^{2}K).

Specifically, when the insulation features of the tank do not allow the external environment to contribute to the heating process of the storage fluid, the amount of produced thermal energy is more strongly influenced by the shape factor S/V.

The influence of the thermal transmittance on the curve concavity is visible in Fig. 9. When U increases, the curve concavity changes from upward to downward.

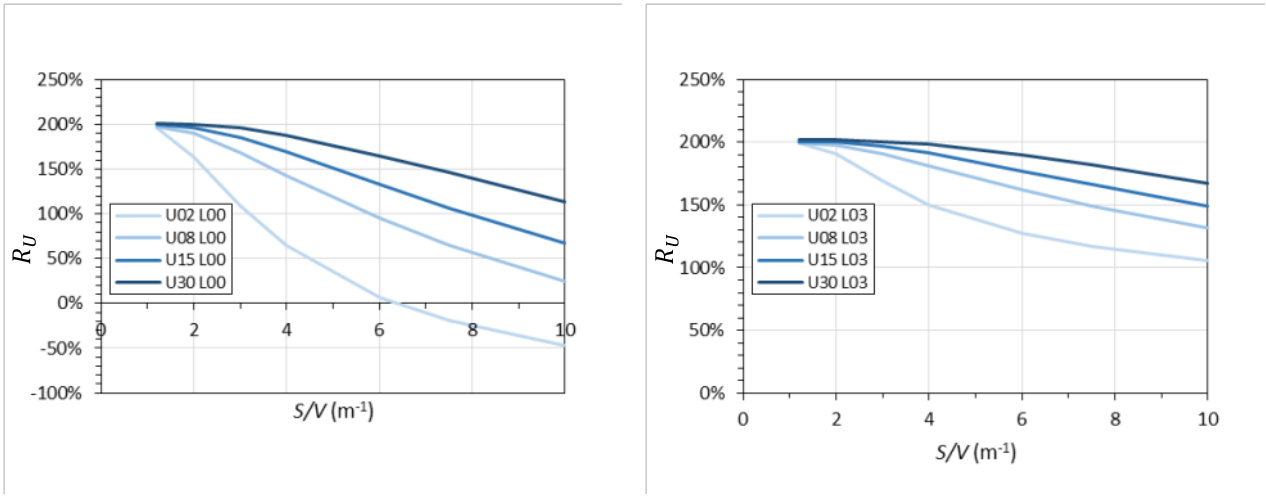

a) b)

Fig. 9. Ratio of the thermal energy production to the electrical energy production of the standard PV system, R_U: case a) no thermal load; case b) thermal load condition L03.

To sum up, Fig. 10 reports the trend of primary energy savings efficiency, referred to different load conditions and tank configurations, *versus* the shape factor *S/V*. The curves show the same profile as the energy production.

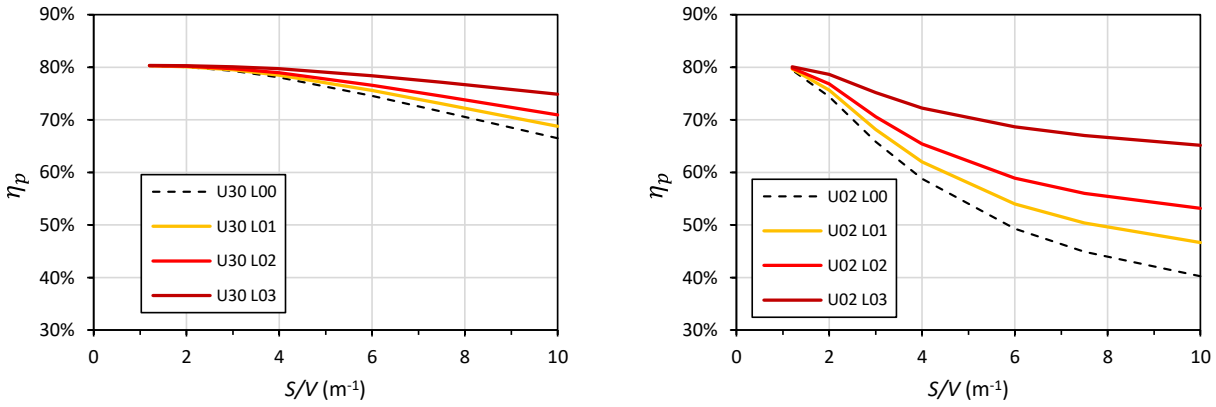

a) b)

Fig. 10. Annual primary energy savings efficiency:
case a) U=3.0 W/m^{2}K; case b) U=0.2 W/m^2/K.

With a view to drawing conclusions about the possible system usability, it is also worth analysing the quality of the generated thermal energy, which can be esteemed as a function of the temperature characterizing the energy production.

From this perspective, information regarding the water storage temperature can be inferred from Figg. 10-14. They report the year fraction f (f_{25} or f_{45}) during which the water storage temperature keeps higher than a fixed value (either 25°C or 45°C) as a function of the shape factor S/V.

Considering that the groundwater temperature was assumed constant and equal to 15°C, the water temperature value of 25°C is considered as representative of those situations where the PV/T systems are only exploited to preheat the thermal fluid. On the contrary, the value of 45°C usually characterizes thermal energy suitable for satisfying domestic hot water demand.

Firstly, it can be noted that both f_{25} and f_{45} increase with S/V. Therefore, albeit the thermal energy production decreases when S/V increases, the quality of the generated energy improves, because higher values of water temperature are maintained for a longer period of time.

For instance, when the most insulated tank is involved (Fig. 11b, U=0.2 W/m^{2}K), a water storage with $S/V > 4\,m^{-1}$ allowed temperatures higher than 25°C to be kept for a period of time wider than 60% of the whole year, also when the highest value of the load (L03, $\boldsymbol{L_{H,h}} = 62\ W$) is considered.

On the contrary, with the least insulated tank (Fig. 11a, U=3.0 W/m^{2}K) the same result is only yielded for $S/V > 8\,m^{-1}$ and $\boldsymbol{L_{H,h}} < 31\ W$.

This means that, albeit a properly insulated tank may reduce the amount of the generated thermal energy (Fig. 8), it contributes to improving the quality of this production, allowing higher values of water temperature to be kept for quite long period of time, also when larger storage volumes are involved.

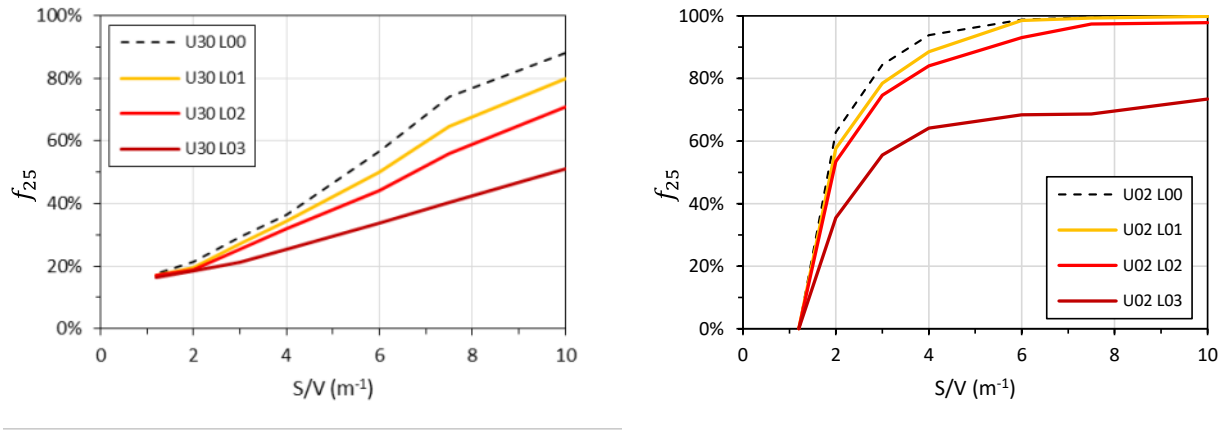

a) b)

Fig. 11. Fraction of time in a year during which the water temperature remains higher than 25°C, f_{25}: case a) U=3.0 W/m^{2}K; case b) U=0.2 W/m^2/K.

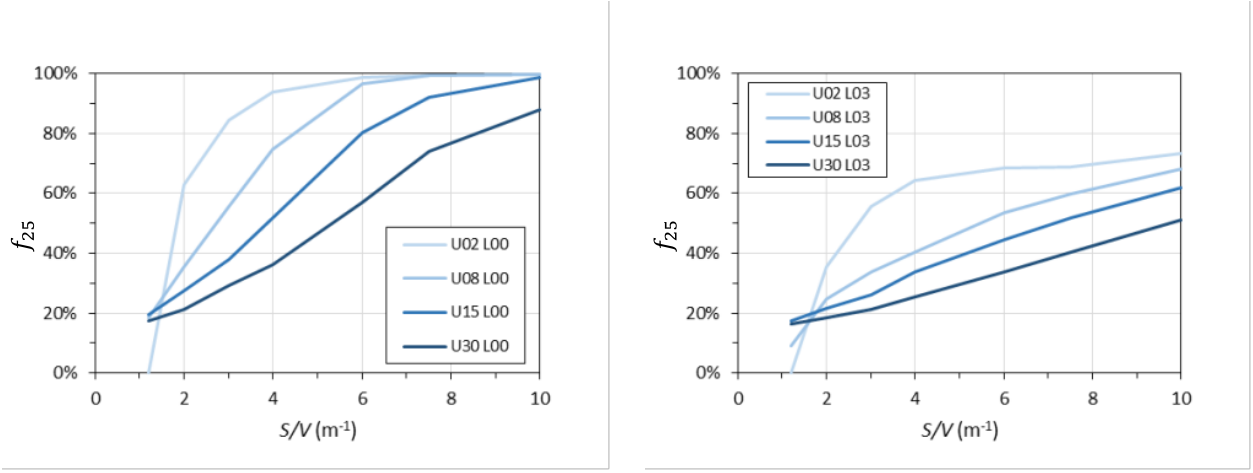

a) b)

Fig. 12. Fraction of time in a year during which the water temperature remains higher than 25°C, f_{25}: case a) no thermal load; case b) thermal load condition L03.

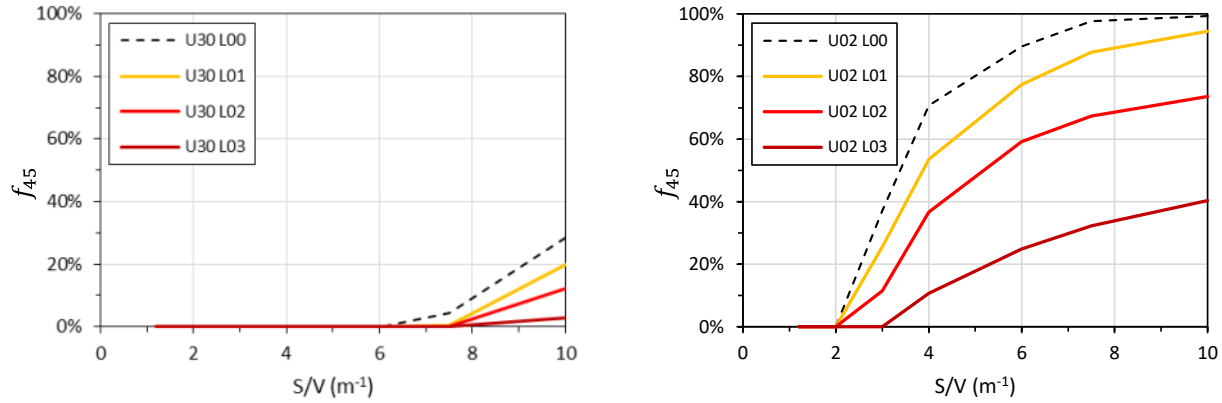

a) b)

Fig. 13. Fraction of time in a year during which the water temperature remains higher than 45°C, f_{45}: case a) U=3.0 W/m^{2}K; case b) U=0.2 W/m^2/K.

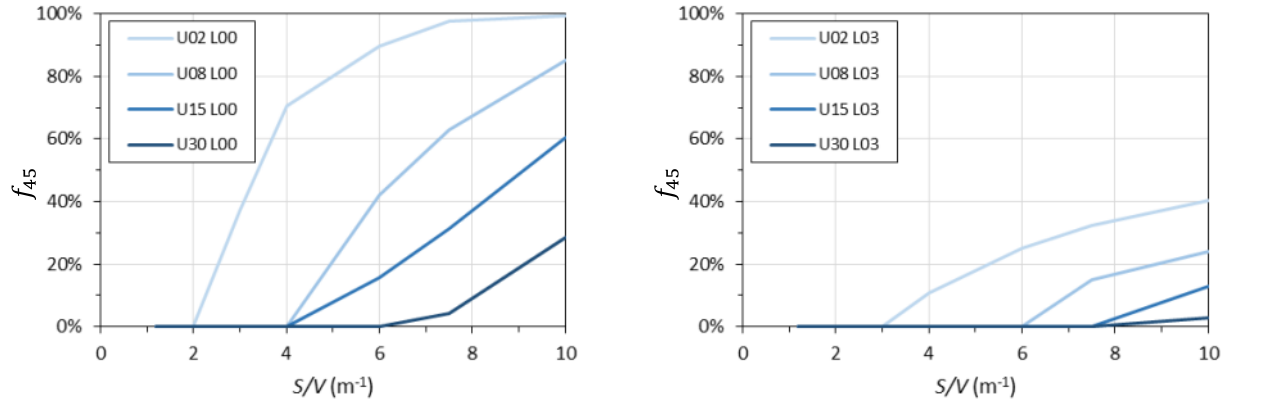

a) b)

Fig. 14. Fraction of time in a year during which the water temperature remains higher than 45°C, f_{45}: case a) no thermal load; case b) thermal load condition L03.

Similar conclusions can be drawn by Fig.15 and Fig. 16, which report the trend of the maximum water storage temperature *versus* S/V.

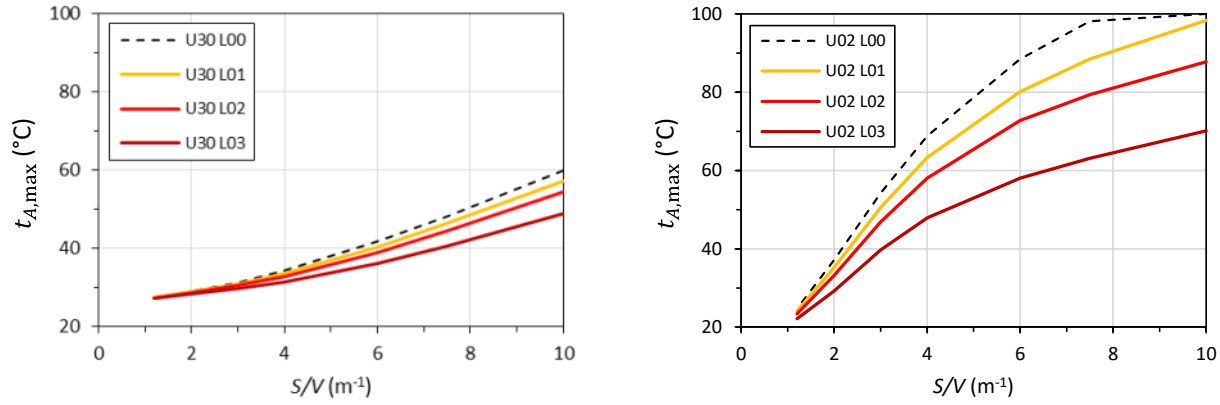

a) b)

436 Fig. 15. Maximum yearly temperature in the storage tank, $t_{A,\max}$: case a) U=3.0 W/m^{2}K; case b) U=0.2 W/m^2/K.

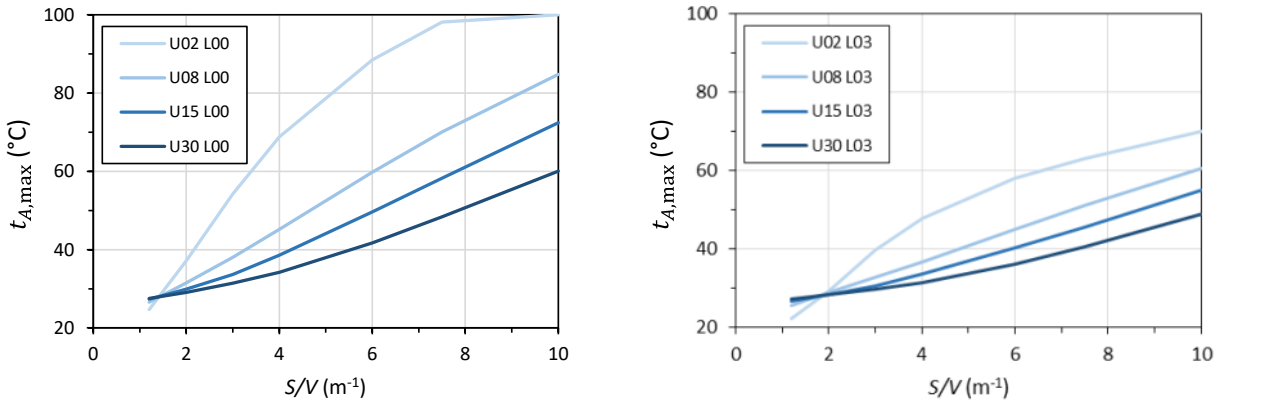

a) b)

437 Fig. 16. Maximum yearly temperature in the storage tank, $t_{A,\max}$: case a) no thermal load; case b) thermal load
438 condition L03.

439 6 Conclusions

440 The paper illustrates the results of a parametric analysis, which aims to provide indications about the
441 influence of the combined interaction of the storage structure (size and thermal transmittance) and the thermal
442 load magnitude on the temperature of the working fluid and, therefore, on the performance of PV/T systems.

443 As a matter of fact, the investigation also regards thermal losses from the storage tank and the possibility
444 of their exploitation to enhance the cooling effect of the PV/T panel, while avoiding remarkable drop of the
445 water storage temperature.

446 Therefore, the analysis presented is also devoted to the quality of the thermal energy, which is attainable
447 and not only to its global amount.

448 However, if a water temperature drop is inevitable in order to guarantee acceptable performances from the
449 PV energy conversion point of view, the parametrical analysis reported in the presented article aims to single
450 out the loads that could be better met in any of the examined cases.

451 These indications can be exploited by designers and researchers to maximize the efficiency of the systems
452 in relation to both electrical and thermal loads and to the features of the water storage.

453 The system has been analytically modelled considering main components and, in order to simulate its
454 performances, a specific code was elaborated and implemented in a spreadsheet, using Visual Basic™ function
455 and macros.

456 Several configurations were patterned and simulated, varying the thermal load and both the thermal
457 insulation properties and dimensions of the tank used for thermal storage purposes. Specifically, the electric
458 and thermal energy production and the storage water temperature have been analysed as a function of the shape
459 factor of the storage tank.

460 Results show that:

461 – the highest increase of the electricity production Δ_E, with respect to the energy production of the standard
462 PV panel working at the same conditions of the analyzed PV/T one, never exceeded 5%, for all the
463 analyzed configurations ($\Delta_E < 5\%$);
464 – for $S/V < 1.8\ m^{-1}$ it was found that $4\% < \Delta_E < 5\%$, regardless the values of the involved parameters
465 (load magnitude, tank transmittance);

466 Therefore, for the sake of electrical production optimization regardless system configurations, storage tanks
467 with small shape factors, $S/V < 1.8\ m^{-1}$, should be used. This condition makes the cooling effect independent
468 from both the tank insulation features and the thermal load magnitude.

469 As regards the thermal energy production, the better performances occur for low values of the shape factor
470 and high thermal loads. However, in this case it is very important to consider the temperature of the water in
471 the thermal storage tank, which should reach appropriate values to be used in HVAC plant or for domestic heat
472 water purpose.

473 The reported results show that small shape factors and poorly insulated tanks do not allow proper values of
474 water temperature to persist for a sufficiently long period of time. The availability of hot water for long periods
475 of time increases with the increase of the shape factor and with the decrease of the thermal transmittance of
476 the tank envelope.

477 Water storage temperature value, only suitable for preheating purposes, higher of 25°C for more than 60%
478 of the whole year ($f_{25} > 60\%$) was obtained for:

479 – $S/V > 2.0\ m^{-1}$, regardless the tank insulation properties, when no thermal load is involved
480 – $S/V > 8.0\ m^{-1}$, regardless the tank insulation properties, when $L_{H,h} = 62\ W$

481 Of course, when meeting the electrical load is the priority, less insulated storage tanks, with smaller shape
482 factors should be preferred, even though it should also be considered that the attainable rise in electrical energy
483 production, with respect to the amount generated by a standard PV panel working at the same condition of the
484 studied PV/T one, never exceeded 5%.

485 On the contrary, when the main goal is the satisfaction of the thermal demand and a high storage water
486 temperature is needed, tanks with high shape factors and low thermal transmittance are more suited to fulfil
487 the purpose. In this case an adequate design of the storage tank could lead to a remarkable improvement of the
488 system thermal performances, with detrimental effect on the PV electrical production, whose value would tend
489 to the one attainable with a standard PV panel. In this case, the PV/T system could also be configured so that
490 it may act as a cogeneration one, although guaranteeing the same electrical energy production as the standard
491 PV panel working at the same conditions.

In conclusion, PV/T systems have a great potential as cogeneration devices, given that electrical and thermal outputs are generated at the same time.

However, attention should be payed to the system features, so that, at least, the performances of a standard PV system are guaranteed, while assuring that thermal energy at a proper temperature is also generated.

From this perspective, the contribution of the analysis to the topic is based on the fact that the performed parametric study can devise general information regarding the possible ranges of values which may be assumed by the variables/parameters used to describe the operation of the system, in correspondence of various conditions.

This could give practical indications about the possible operational regimes of the system depending on the features of the tank and the magnitude of the load.

For example, when the load magnitude is known, results of the analysis can be used for a rough sizing of the tank, selecting a shape factor able to take into account both the perspectives of electric and thermal energy production.

Therefore, the results of the analysis proposed here may provide useful information, even though additional research is also needed to draw definitive conclusions on this topic, especially when economic considerations are involved or the effects of the climatic conditions are considered. In this direction, the development of the research is being planned.

In addition, a comparison with experimental data will be also the future development of the research activity and, to reach this aim, an experimental apparatus is going to be realized at the Mediterranean university campus.

7 Nomenclature

Δ_E	increase of the electric energy production due to the use of the PV/T system respect to a standard PV one
f_{25}	fraction of time in a year during which the water temperature remains higher than 25°C
f_{45}	fraction of time in a year during which the water temperature remains higher than 45°C
$\dot{G}$	water flow of the fluid in the PV/T system (kg/s).
$\dot{G}_{HW}$	water flow of the fluid in demand loop (kg/s).
I_β	solar irradiance on the panel surface (W/m^2);
$NOCT$	Nominal Operating Cell Temperature (°C);
$\dot{Q}_D^\tau$	thermal flow, which is discarded into the environment through the envelope structure of the water storage (W);
$\dot{Q}_E^\tau$	generated electrical power (W);
$\dot{Q}_T^\tau$	generated thermal power (W);
$\dot{Q}_U^\tau$	global available thermal power, namely the power which is globally at the load disposal (W);
$\dot{Q}_{ue}^\tau$	effective thermal power, namely the thermal power which is actually sent to the thermal load (W);
L_H	yearly thermal load (kWh);
$Q_{E,PV}$	yearly electrical energy, generated by the PV panel characterized by the same features as the studied PV/T one and working at the same conditions (kWh);
$Q_{E,PV/T}$	yearly electrical energy, generated by the PV/T panel (kWh);
Q_U	yearly available thermal energy, at load disposal (kWh);
S_p	area of the panel surface (m^2);
R_U	ratio of the thermal energy production to the electrical energy production of the standard PV system (non-dimens.);

R_E	ratio of the electrical energy production due to the use of the PV/T system respect to a standard PV one (non-dimens.);
t_a	air temperature (°C);
$t_{F,A}$	storage temperature (°C);
$t_{F,basin}$	groundwater temperature (°C);
$t_{c,PV}$	cell temperature of a standard PV system operating at the same condition of the actual PV/T plant (°C);
$t_{c,PV/T}$	actual cell temperature of the PV/T collector (°C);
$t_{F,A}$	water temperature in the storage system (°C);
$t_{F,iA}$	inlet water temperature to the storage system (°C);
$t_{F,oA}$	outlet water temperature of the water storage (°C);
$t_{F,iC}$	inlet water temperature to the collector (°C);
$t_{F,oC}$	outlet water temperature from the collector (°C);
t_p	temperature of the absorber plate (°C);
Δ_E	increase of the electric energy production due to the use of the PV/T system respect to a standard PV one;
η_p	primary energy saving efficiency (non-dimens.);
η_e	electrical power generation efficiency of the Italian energy system (non-dimens.);
η_r	nominal efficiency of the PV panel (non-dimens.);
β	temperature coefficient of the panel (%°C^{-1});
η_{PV}	electrical efficiency (non-dimens.);
η_0, k_1, k_2	parameters characterizing the thermal collector (non-dimens.);
η_T	thermal efficiency (non-dimens.).

8 Acknowledgement

This work was carried out within the research project n. 201594LT3F, "*La ricerca per i PAES: una piattaforma per le municipalità partecipanti al Patto dei Sindaci (Research for SEAP: a platform for municipalities taking part in the Covenant of Mayors)*", which is funded by the PRIN (Programmi di Ricerca Scientifica di Rilevante Interesse Nazionale) of the Italian Ministry of Education, University and Research.

9 References

[1] J.J. Michael, I. S, R. Goic, Flat plate solar photovoltaic-thermal (PV/T) systems: A reference guide, Renew. Sustain. Energy Rev. 51 (2015) 62–88. https://doi.org/10.1016/j.rser.2015.06.022.

[2] N.L. Panwar, S.C. Kaushik, S. Kothari, Role of renewable energy sources in environmental protection: A review, Renew. Sustain. Energy Rev. 15 (2011) 1513–1524. https://doi.org/10.1016/j.rser.2010.11.037.

[3] International Energy Agency (IEA), Solar PV, (2018) 1–7. https://www.iea.org/tcep/power/renewables/solar/ (accessed November 12, 2018).

[4] M.A. Hasan, K. Sumathy, Photovoltaic thermal module concepts and their performance analysis: A review, Renew. Sustain. Energy Rev. 14 (2010) 1845–1859. https://doi.org/10.1016/j.rser.2010.03.011.

[5] S.S. Joshi, A.S. Dhoble, Photovoltaic -Thermal systems (PVT): Technology review and future trends, Renew. Sustain. Energy Rev. 92 (2018) 848–882. https://doi.org/10.1016/j.rser.2018.04.067.

[6] E. Skoplaki, J.A. Palyvos, On the temperature dependence of photovoltaic module electrical performance: A review of efficiency/power correlations, Sol. Energy. 83 (2009) 614–624. https://doi.org/https://doi.org/10.1016/j.solener.2008.10.008.

[7] A. Shukla, K. Kant, A. Sharma, P.H. Biwole, Cooling methodologies of photovoltaic module for enhancing electrical efficiency: A review, Sol. Energy Mater. Sol. Cells. 160 (2017) 275–286. https://doi.org/https://doi.org/10.1016/j.solmat.2016.10.047.

[8] M.Y. AbuGrain, H.Z. Alibaba, Optimizing existing multistory building designs towards net-zero energy, Sustain. 9 (2017). https://doi.org/10.3390/su9030399.

[9] S. Attia, P. Eleftheriou, F. Xeni, R. Morlot, C. Ménézo, V. Kostopoulos, M. Betsi, I. Kalaitzoglou, L. Pagliano, M. Cellura, M. Almeida, M. Ferreira, T. Baracu, V. Badescu, R. Crutescu, J.M. Hidalgo-Betanzos, Overview and future challenges of nearly Zero Energy Buildings (nZEB) design in Southern Europe, Energy Build. 155 (2017) 439–458. https://doi.org/10.1016/j.enbuild.2017.09.043.

[10] D. Chemisana, E.F. Fernandez, A. Riverola, A. Moreno, Fluid-based spectrally selective filters for direct immersed PVT solar systems in building applications, Renew. Energy. 123 (2018) 263–272. https://doi.org/https://doi.org/10.1016/j.renene.2018.02.018.

[11] U.J. Rajput, J. Yang, Comparison of heat sink and water type PV/T collector for polycrystalline photovoltaic panel cooling, Renew. Energy. 116 (2018) 479–491. https://doi.org/10.1016/j.renene.2017.09.090.

[12] V. V. Tyagi, S.C. Kaushik, S.K. Tyagi, Advancement in solar photovoltaic/thermal (PV/T) hybrid collector technology, Renew. Sustain. Energy Rev. 16 (2012) 1383–1398. https://doi.org/10.1016/j.rser.2011.12.013.

[13] A. Gagliano, G.M. Tina, F. Nocera, A.D. Grasso, S. Aneli, Description and performance analysis of a flexible photovoltaic/thermal (PV/T) solar system, Renew. Energy. 137 (2019) 144–156. https://doi.org/10.1016/j.renene.2018.04.057.

[14] F. Sarhaddi, S. Farahat, H. Ajam, A. Behzadmehr, M. Mahdavi Adeli, An improved thermal and electrical model for a solar photovoltaic thermal (PV/T) air collector, Appl. Energy. 87 (2010) 2328–2339. https://doi.org/10.1016/j.apenergy.2010.01.001.

[15] S.Y. Wu, C. Chen, L. Xiao, Heat transfer characteristics and performance evaluation of water-cooled PV/T system with cooling channel above PV panel, Renew. Energy. 125 (2018) 936–946. https://doi.org/10.1016/j.renene.2018.03.023.

[16] P. Dupeyrat, C. Ménézo, M. Rommel, H.M. Henning, Efficient single glazed flat plate photovoltaic-thermal hybrid collector for domestic hot water system, Sol. Energy. 85 (2011) 1457–1468. https://doi.org/10.1016/j.solener.2011.04.002.

[17] N. Aste, C. del Pero, F. Leonforte, Water flat plate PV-thermal collectors: A review, Sol. Energy. 102 (2014) 98–115. https://doi.org/10.1016/j.solener.2014.01.025.

[18] P. Dupeyrat, C. Ménézo, H. Wirth, M. Rommel, Improvement of PV module optical properties for PV-thermal hybrid collector application, Sol. Energy Mater. Sol. Cells. 95 (2011) 2028–2036. https://doi.org/10.1016/j.solmat.2011.04.036.

[19] C. Lamnatou, D. Chemisana, Photovoltaic/thermal (PVT) systems: A review with emphasis on environmental issues, Renew. Energy. 105 (2017) 270–287. https://doi.org/10.1016/j.renene.2016.12.009.

[20] S.S. Joshi, A.S. Dhoble, Photovoltaic -Thermal systems (PVT): Technology review and future trends, Renew. Sustain. Energy Rev. 92 (2018) 848–882. https://doi.org/10.1016/j.rser.2018.04.067.

[21] H.A.K. and M.T.C. Ali H. A. Al-Waeli, K. Sopian, Photovoltaic / Thermal (PV / T) Systems, Int. J. Comput. Appl. Sci. 2 (2017) 62–67.

[22] A. Zarrella, G. Emmi, J. Vivian, L. Croci, G. Besagni, The validation of a novel lumped parameter model for photovoltaic thermal hybrid solar collectors: a new TRNSYS type, Energy Convers. Manag. 188 (2019) 414–428. https://doi.org/10.1016/j.enconman.2019.03.030.

[23] S.A. Kalogirou, R. Agathokleous, G. Barone, A. Buonomano, C. Forzano, A. Palombo, Development

and validation of a new TRNSYS Type for thermosiphon flat-plate solar thermal collectors: energy and economic optimization for hot water production in different climates, Renew. Energy. 136 (2019) 632–644. https://doi.org/10.1016/j.renene.2018.12.086.

[24] F. Calise, M.D. D'Accadia, L. Vanoli, Design and dynamic simulation of a novel solar trigeneration system based on hybrid photovoltaic/thermal collectors (PVT), Energy Convers. Manag. 60 (2012) 214–225. https://doi.org/10.1016/j.enconman.2012.01.025.

[25] S. Sanaye, A. Sarrafi, Optimization of combined cooling, heating and power generation by a solar system, Renew. Energy. 80 (2015) 699–712. https://doi.org/10.1016/j.renene.2015.02.043.

[26] M. Herrando, A.M. Pantaleo, K. Wang, C.N. Markides, Solar combined cooling, heating and power systems based on hybrid PVT, PV or solar-thermal collectors for building applications, Renew. Energy. 143 (2019) 637–647. https://doi.org/10.1016/j.renene.2019.05.004.

[27] M. Herrando, A. Ramos, J. Freeman, I. Zabalza, C.N. Markides, Technoeconomic modelling and optimisation of solar combined heat and power systems based on flat-box PVT collectors for domestic applications, Energy Convers. Manag. 175 (2018) 67–85. https://doi.org/10.1016/j.enconman.2018.07.045.

[28] M.A. Cucumo, V. Marinelli, G. Oliveti, Ingegneria solare. Principi ed applicazioni, Pitagora Editrice, Bologna, 1994.

[29] S. Bhattarai, G.K. Kafle, S.H. Euh, J.H. Oh, D.H. Kim, Comparative study of photovoltaic and thermal solar systems with different storage capacities: Performance evaluation and economic analysis, Energy. 61 (2013) 272–282. https://doi.org/10.1016/j.energy.2013.09.007.

[30] Ministry of Economic Development, Ministry of the Environment, Ministry of Infrastructure and Transportation systems, Decreto interministeriale 26 giugno 2015 - Applicazione delle metodologie di calcolo delle prestazioni energetiche e definizione delle prescrizioni e dei requisiti Ministry of Economic Development minimi degli edifici, Rome, 2015.

[31] J.A. Duffie, W.A. Beckman, Solar Engineering of Thermal Processes, John Wiley & Sons, Inc., Hoboken, NJ, USA, 2013. https://doi.org/10.1002/9781118671603.

[32] D. Evans, Simplified method for predicting PV array output., Sol. Energy. 27 (1981) 555–560. https://doi.org/https://doi.org/10.1016/0038-092X(81)90051-7Get.

[33] N. Aste, F. Leonforte, C. Del Pero, Design, modeling and performance monitoring of a photovoltaic-thermal (PVT) water collector, Sol. Energy. 112 (2015) 85–99. https://doi.org/10.1016/j.solener.2014.11.025.

[34] B.Y.H. Liu, R.C. Jordan, The interrelationship and characteristic distribution of direct, diffuse and total solar radiation, Sol. Energy. 4 (1960) 1–19. https://doi.org/10.1016/0038-092X(60)90062-1.

[35] J.A. Duffie, W.A. Beckman, Solar Engineering of Thermal Processes, 2006.

[36] G. Evola, C. Marino, M.F. Panzera, M. Infantone, L. Marletta, Upgrading weather datasets for building energy simulation : a preliminary investigation, in: Accept. to 20th Int. Conf. Environ. Electr. Eng. (EEEIC 2020), 2020.

[37] L. Cirrincione, C. Malara, C. Marino, A. Nucara, G. Peri, M. Pietrafesa, PV/T Systems: Effect of both storage features and load configuration, in: Proc. Build. Simul. 2019 16th Conf., International Building Performance Association (IBPSA)., Rome, 2019.